MITSUBISHI ELECTRIC RESEARCH LABORATORIES
http://www.merl.com

Dynamic State Estimation Based on Unscented Kalman Filter and Very Short-Term Load and Distributed Generation Forecasting

Sun, H.; Feng, G.; Nikovski, D.N.

TR2016-128 September 2016

Abstract

This paper proposes an unscented Kalman filter (UKF) based dynamic state estimation (DSE) method for distribution systems by incorporating very short-term load and distributed generation (DG) forecasting. Instead of fitting state variables into unrealistic state transition models for the prediction step in UKF, this work forecasts and transforms nodal power injections from both load and DG into state predictions through load flow computation. The impact of bad data and irrational sigma points are mitigated through the sanity check and adjustment to the power injections. The test results on a modified IEEE 123-node test feeder are given to demonstrate the effectiveness of the proposed method.

POWERCON

Dynamic State Estimation Based on Unscented Kalman Filter and Very Short-Term Load and Distributed Generation Forecasting

Hongbo Sun
Mitsubishi Electric Research Laboratories,
Cambridge, MA 02139, USA

Guangyu Feng
Dept. of Electrical Engineering,
Northeastern University,
Boston, MA 02115, USA

Daniel Nikovski, Jinyun Zhang
Mitsubishi Electric Research Laboratories,
Cambridge, MA 02139, USA

***Abstract*--This paper proposes an unscented Kalman filter (UKF) based dynamic state estimation (DSE) method for distribution systems by incorporating very short-term load and distributed generation (DG) forecasting. Instead of fitting state variables into unrealistic state transition models for the prediction step in UKF, this work forecasts and transforms nodal power injections from both load and DG into state predictions through load flow computation. The impact of bad data and irrational sigma points are mitigated through the sanity check and adjustment to the power injections. The test results on a modified IEEE 123-node test feeder are given to demonstrate the effectiveness of the proposed method.**

***Index Terms*--Distributed generation, Dynamic state estimation, Short-term load forecasting, Unscented Kalman filter.**

I. INTRODUCTION

Dynamic state estimation (DSE) differs with static state estimation in that it uses memory of previous state and state transition model to predict the next state and then filters it with the measurement model. Earlier works on DSE [1]–[3] have applied the extended Kalman filter (EKF), which tackles nonlinear systems through first order linear approximation. The iterated Kalman filter (IKF) improves the accuracy of EKF by iteratively updating the state variables [4], while significantly increasing computational burden. For high-order non-linear systems, EKF might introduce large approximation errors. This issue is addressed by usage of the unscented Kalman filter (UKF) which can approximate the posterior mean and covariance accurately to the 3rd order Taylor series expansion [5]. UKF has been introduced to the area of DSE for power systems by [6]-[7] and is getting increased attention.

The implementation of Kalman filters, however, requires a state transition model in addition to measurement model to be available. The state transition model is necessary for the prediction step in Kalman filters. Depending on how the state transition model is built or the state is predicted, there are roughly three kinds of DSE methods: the ones creating explicit state equations from discretized differential equations of generators [7]-[9], the ones directly approximating state transition models with various assumptions [6], [10]–[12], and the ones transforming load forecasts into state forecasts through load flow computation [1], [2], [13].

With the increasing deployment of advanced measurement systems, such as PMUs in power systems, the estimation of electromagnetic dynamics of generators such as rotor speeds and angles becomes feasible. The works in [7]-[9] assume fast update rate in the level of milliseconds and use numerical integration or Runga-Kutta method to transform the differential equations of generators to state space equations. Those kind of methods, however, is hard to be regarded as general purpose state estimators since they have to assume known models of loads as well as other complex components, furthermore, the scale of their state equations will grow significantly in the cases of realistic large power systems.

As for the DSE methods estimating bus voltage phasor, in the earliest DSE work [10], the authors used EKF and represented the state update by the over-simplified random walk model. The work in [11] improved the EKF based DSE by forecasting the state through exponential smoothing techniques, to be more specific, the Holt's double exponential smoothing method. A detailed comparison of several state prediction methods can be found in [3]. The application of UKF in DSE was proposed in [6] where the authors also used exponential smoothing method as in [11] for predicting state variables.

Nevertheless, the fitting of state transition model suffers from lack of physical meaning and often neglects the dependence between state variables [3]. A comparatively more realistic approach is to model the more inter-independent variation of nodal power injections that actually drive the system dynamics. The authors of [1] introduced ANN based load forecasting to EKF based DSE. In [13], IKF is used to gain better accuracy over EKF, and actual injections based on load profile is used as "load forecasts" for predicting the state variables. So far, no practice has been found incorporating load forecasting into UKF based DSE.

In this paper, an UKF based dynamic state estimation method is proposed for distribution systems by incorporating very short-term power injection forecasting. Instead of fitting state variables into unrealistic state transition models, the proposed method forecasts and transforms nodal power injections from both load and DG into state predictions through load flow computation. Through integrating UKF based DSE with DG and load forecasting, the power injections that drive the changes of system states can be predicted more precisely, and accordingly more accurate state estimation can be obtained. The trade-off of power injection forecasting aided DSE is the increased computation burden caused by the load flow evaluation after each injection forecast. Considered the radial configuration of most distribution systems, the increased computation can be effectively reduced by using more efficient load flow algorithms such as the backward/forward sweep methods [14]-[15]. Meanwhile, the estimation accuracy is further improved by mitigating the impacts of bad data and irrational sigma points through the sanity check and adjustment of nodal injections.

The rest of this paper is organized as follows: section II briefly describes the technical background, i.e., procedures for UKF based DSE and exponential smoothing methods for load and DG injection forecasting; section III explains in detail how load and DG injection forecasting is embedded to the estimation procedure, and section IV discusses the special consideration for distribution systems; then section V demonstrates the estimation results for test systems under fluctuating load and DG injections. Finally section VI presents the conclusions of this work.

II. Preliminaries on UKF Based DSE and Exponential Smoothing Algorithms

For a distribution system, its state transition model and measurement model can be described as follows:

$$\mathbf{x}_k = \mathbf{f}(\mathbf{x}_{k-1}, k-1) + \mathbf{q}_{k-1}, \tag{1}$$

$$\mathbf{y}_k = \mathbf{h}(\mathbf{x}_k, k) + \mathbf{r}_k, \tag{2}$$

where, $\mathbf{x}_k$ and $\mathbf{y}_k$ are the vectors of states and measurements at time interval k, $\mathbf{q}_k$ and $\mathbf{r}_k$ are the Gaussian noises for states and measurements at time interval k, with zero means and diagonal covariance matrices $\mathbf{Q}_k$ and $\mathbf{R}_k$ respectively. This work only studies the dynamic state estimation for network states, i.e. voltage phasors, and the generator states, e.g. rotor angles and frequencies, are not in the scope of this work.

A. UKF based DSE

For each time interval k, the UKF based DSE can be implemented through three major steps, including sigma point calculation, state prediction and state correction [6].

The sigma-point calculation step uses the estimate of state variables at interval (k-1), $\hat{\mathbf{x}}_{k-1}$ and the corresponding covariance matrix, $\mathbf{P}_{k-1}$ to create a set of ($2n_s$ +1) sigma points, $\mathbf{X}_{k-1}$ according to:

$$\mathbf{X}_{k-1} = \left[\hat{\mathbf{x}}_{k-1} \ \ldots \ \hat{\mathbf{x}}_{k-1}\right] + \sqrt{(n_s+\lambda)}\left[0 \ \ \sqrt{\mathbf{P}_{k-1}} \ \ -\sqrt{\mathbf{P}_{k-1}}\right], \tag{3}$$

where, n_s is the dimension of state variables, $\lambda = \alpha_s^2(n_s+\kappa) - n_s$, α_s and κ are the parameters that determine the spread of the sigma points around. The square root of the covariance matrix $\mathbf{P}_{k-1}$ can be solved using the Cholesky factorization method.

In the step of state prediction, the sigma points $\mathbf{X}_{k-1}$ are propagated column by column through the state transition model in (1) to generate $\hat{\mathbf{X}}_k$ so as to predict the next state $\hat{\mathbf{x}}_k^-$ and covariance matrix, $\mathbf{P}_k^-$ according to:

$$\hat{\mathbf{x}}_k^- = \sum_{l=0}^{2n_s} \mathbf{W}_l^m \hat{\mathbf{X}}_k^l, \tag{4}$$

$$\mathbf{P}_k^- = \sum_{l=0}^{2n_s} \mathbf{W}_l^c \left[\left(\hat{\mathbf{X}}_k^l - \hat{\mathbf{x}}_k^-\right)\left(\hat{\mathbf{X}}_k^l - \hat{\mathbf{x}}_k^-\right)^T\right] + \mathbf{Q}_{k-1}, \tag{5}$$

$$\hat{\mathbf{X}}_k^l = \mathbf{f}(\mathbf{X}_{k-1}^l, \mathbf{k}-1), \tag{6}$$

where, $\mathbf{X}_{k-1}^l$ and $\hat{\mathbf{X}}_k^l$ are the l-th columns of $\mathbf{X}_{k-1}$ and $\hat{\mathbf{X}}_k$ respectively, $\mathbf{W}_0^c = \lambda/(n_s+\lambda) + 1 - \alpha_s^2 + \beta_s$, $\mathbf{W}_0^m = \lambda/(n_s+\lambda)$, $\mathbf{W}_l^m = \mathbf{W}_l^c = 0.5/(n_s+\lambda)$, β_s is a parameter to incorporate prior knowledge of the distribution of state variable. The state correction step uses the predicted state, $\hat{\mathbf{x}}_k^-$ and covariance matrix, $\mathbf{P}_k^-$ to calculate the corresponding sigma points, $\mathbf{X}_k^-$:

$$\mathbf{X}_k^- = \left[\hat{\mathbf{x}}_k^- \ \ldots \ \hat{\mathbf{x}}_k^-\right] + \sqrt{(n_s+\lambda)}\left[0 \ \ \sqrt{\mathbf{P}_k^-} \ \ -\sqrt{\mathbf{P}_k^-}\right]. \tag{7}$$

Then sigma points $\mathbf{X}_k^-$ are propagated column by column through the measurement equation in (2) to compute the Kalman filter gain $\mathbf{K}_k$ by which the predicted state and covariance matrix are corrected to generate the estimated state $\hat{\mathbf{x}}_k$ and $\mathbf{P}_k$ according to:

$$\hat{\mathbf{x}}_k = \hat{\mathbf{x}}_k^- + \mathbf{K}_k\left[\mathbf{y}_k - \hat{\mathbf{y}}_k^-\right], \tag{8}$$

$$\mathbf{P}_k = \mathbf{P}_k^- - \mathbf{K}_k \mathbf{P}_{Y_kY_k} \mathbf{K}_k^T, \tag{9}$$

$$\mathbf{K}_k = \mathbf{P}_{X_kY_k} \mathbf{P}_{Y_kY_k}^{-1}, \tag{10}$$

$$\hat{\mathbf{y}}_k^- = \sum_{l=0}^{2n_s} \mathbf{W}_l^m \mathbf{Y}_k^{-l}, \tag{11}$$

$$\mathbf{Y}_k^- = \mathbf{h}(\mathbf{X}_k^-, k), \tag{12}$$

$$\mathbf{P}_{Y_kY_k} = \sum_{l=0}^{2n_s} \mathbf{W}_l^c \left[\left(\mathbf{Y}_k^{-l} - \hat{\mathbf{y}}_k^-\right)\left(\mathbf{Y}_k^{-l} - \hat{\mathbf{y}}_k^-\right)^T\right] + \mathbf{R}_k, \tag{13}$$

$$\mathbf{P}_{X_kY_k} = \sum_{l=0}^{2n_s} \mathbf{W}_l^c \left[\left(\mathbf{X}_k^{-l} - \hat{\mathbf{x}}_k^-\right)\left(\mathbf{Y}_k^{-l} - \hat{\mathbf{y}}_k^-\right)^T\right], \tag{14}$$

where, $\mathbf{Y}_k^{-l}$ is the l-th column of $\mathbf{Y}_k^-$.

As shown in (6), the evaluation of the sigma points involves transforming each column in $\mathbf{X}_{k-1}$ to a column at the same location in $\hat{\mathbf{X}}_k$ through the function $\mathbf{f}(\mathbf{x}_{k-1}, k-1)$ which is a time-varying implicit non-linear function. The conventional UKF estimation procedures commonly use direct/explicit state transition models. Instead, this work uses an indirect state transition model to predict state variables through injection forecasting and load flow computation.

B. Exponential Smoothing Algorithms

When the historical data and related information such as weather data are available, the future loads and distributed generations can be forecasted through a suitable forecasting technique. The survey in [16] reveals that for very short term (less than 5 minutes) load forecasting, it is unnecessary to adopt complicated forecasting techniques such as the ones considering multiple seasonalities. In this work, the exponential smoothing techniques [17] that commonly used for very short-term load forecasting are employed to determine the nodal power injections contributed by loads and DGs. Due to the short intervals of load and DG forecasting, only single and double exponential smoothing algorithms are used.

1) Single Exponential Smoothing: The single exponential smoothing (SES) has only one smoothing constant as shown in below:

$$\mathbf{S}_{k+1}^- = \alpha_f \hat{\mathbf{S}}_k + \left(1-\alpha_f\right)\mathbf{S}_k^-, \ 0 \le \alpha_f \le 1, \tag{15}$$

where, $\mathbf{S}_{k+1}^-$ is the injection forecast at interval k for the next interval (k + 1), and $\hat{\mathbf{S}}_k$ is the measured/forecasted injection at step k or calculated injection based on the estimated state at step k, α_f is the smoothing factor. As shown in (15), the new forecast for time interval (k + 1) is determined as a weighted linear combination of previous forecast $\mathbf{S}_k^-$ and new observation at time interval k, $\hat{\mathbf{S}}_k$.

2) Double Exponential Smoothing: If there is a trend in the time series data, double exponential smoothing (DES) is used to include an additional parameter representing the trend in the data. The Holt-Winters double exponential smoothing is used in this work, and its formulas are:

$$\mathbf{S}_{k+1}^{-} = \mathbf{L}_k + \mathbf{T}_k , \tag{16}$$

$$\mathbf{L}_k = \alpha_f \hat{\mathbf{S}}_k + (1-\alpha_f)(\mathbf{L}_{k-1} + \mathbf{T}_{k-1}),\ 0 \le \alpha_f \le 1 ,$$
$$\mathbf{T}_k = \beta_f (\mathbf{L}_k - \mathbf{L}_{k-1}) + (1-\beta_f)\mathbf{T}_{k-1} , 0 \le \beta_f \le 1 , \tag{17}$$

where, $\mathbf{L}_k$ and $\mathbf{T}_k$ represent the level and trend of the data at time interval k, α_f and β_f are the first and second smoothing constants. The initial vales for levels and trends are set as: $\mathbf{L}_1 = \hat{\mathbf{S}}_1$, $\mathbf{T}_1 = \hat{\mathbf{S}}_2 - \hat{\mathbf{S}}_1$.

III. Propsed Procedure for UKF-based DSE Integrating Injection Forecasting And Load Flow

This work proposes jointly using UKF and very short-term power injection forecasting to implement DSE for three-phase distribution systems. The state transitions are indirectly modelled through load and DG forecasting and load flow computation. In addition, the sanity check and adjustment of injections is used to mitigate the impacts of bad data or irrational sigma points on the estimation accuracy.

For an arbitrary time interval *k*, the proposed dynamic state estimation method can be illustrated by the following procedure:

1) Calculate sigma points $\mathbf{X}_{k-1}$ based on the estimated state and covariance matrix at time interval (*k*-1), $\hat{\mathbf{x}}_{k-1}$ and $\mathbf{P}_{k-1}$ using (3).
2) Set the sigma point counter *l* as 1, i.e. *l*=1.
3) Based on the *l*-th column of $\mathbf{X}_{k-1}$, $\mathbf{X}_{k-1}^{l}$, determine a calculated injection vector $\widetilde{\mathbf{S}}_{k-1}^{l}$ using nodal power injection equations.
4) Use $\widetilde{\mathbf{S}}_{k-1}^{l}$ and historical injection data to forecast a calculated injection at time interval *k*, $\widetilde{\mathbf{S}}_{k}^{l}$ according to (18) if SES is used, or (19) if DES is used.

$$\widetilde{\mathbf{S}}_k^l = \alpha_f \widetilde{\mathbf{S}}_{k-1}^l + \left(1-\alpha_f\right)\mathbf{S}_{k-1}^{-} , \tag{18}$$

$$\widetilde{\mathbf{S}}_k^l = \widetilde{\mathbf{L}}_{k-1}^l + \widetilde{\mathbf{T}}_{k-1}^l ,$$
$$\widetilde{\mathbf{L}}_{k-1}^l = \alpha_f \widetilde{\mathbf{S}}_{k-1}^l + (1-\alpha_f)(\mathbf{L}_{k-2} + \mathbf{T}_{k-2}) ,$$
$$\widetilde{\mathbf{T}}_{k-1}^l = \beta_f (\mathbf{L}_{k-1} - \mathbf{L}_{k-2}) + (1-\beta_f)\mathbf{T}_{k-2} . \tag{19}$$

5) Check the sanity of the calculated injections at time interval *k*, $\widetilde{\mathbf{S}}_k^l$ against a set of upper and lower bounds, $\overline{\widetilde{\mathbf{S}}}_k$ and $\underline{\widetilde{\mathbf{S}}}_k$ defined based on the injection forecasts at interval (*k*-1), $\hat{\mathbf{S}}_{k-1}$ and associated standard deviations, $\boldsymbol{\sigma}_{k-1}$:

$$\overline{\widetilde{\mathbf{S}}}_k = \hat{\mathbf{S}}_{k-1} + \gamma \boldsymbol{\sigma}_{k-1} ,$$
$$\underline{\widetilde{\mathbf{S}}}_k = \hat{\mathbf{S}}_{k-1} - \gamma \boldsymbol{\sigma}_{k-1} , \tag{20}$$

where, γ is a pre-determined parameter that determines the reasonable ranges of power injection variations caused by forecasting errors and injection changes between intervals. The calculated injections will be adjusted to be within the corresponding bounds if their values are beyond the upper or lower bounds according to:

$$\widetilde{\mathbf{S}}_k^l = \overline{\widetilde{\mathbf{S}}}_k \text{ , if } \widetilde{\mathbf{S}}_k^l > \overline{\widetilde{\mathbf{S}}}_k ,$$
$$\widetilde{\mathbf{S}}_k^l = \underline{\widetilde{\mathbf{S}}}_k \text{ , if } \widetilde{\mathbf{S}}_k^l < \underline{\widetilde{\mathbf{S}}}_k . \tag{21}$$

6) Run load flow program to determine a corresponding state estimation for interval *k*, $\hat{\mathbf{X}}_k^l$ by taken the determined power injection $\widetilde{\mathbf{S}}_k^l$ as the nodal power injections.
7) Check whether all sigma points are propagated, i.e. $l == (2n_s + 1)$, if yes, go to 8); otherwise, set $l = l + 1$, and go to 3).
8) Predict state and covariance for time interval *k*, $\hat{\mathbf{x}}_k^{-}$ and $\mathbf{P}_k^{-}$ based on $\hat{\mathbf{X}}_k$ according to (4) and (5), and then determine their corresponding sigma points $\mathbf{X}_k^{-}$ using (7).
9) Propagate $\mathbf{X}_k^{-}$ with the measurement function to determine the Kalman gain $\mathbf{K}_k$ according to (10)-(14).
10) Read the measurements at time interval *k*, $\mathbf{y}_k$ and correct predicted $\hat{\mathbf{x}}_k^{-}$ and covariance matrix $\mathbf{P}_k^{-}$ with $\mathbf{K}_k$ to generate the estimated $\hat{\mathbf{x}}_k$ and $\mathbf{P}_k$ using (8)-(9).
11) Read the load and distributed generation forecasts or measurements at time interval *k*, and determine corresponding nodal power injections, $\hat{\mathbf{S}}_k$, if the load and distributed generation forecasts are available. Otherwise, based on $\hat{\mathbf{x}}_k$, determine the calculated nodal power injections, $\hat{\mathbf{S}}_k$ using nodal power flow equations.
12) Determine the predicted nodal power injections for time interval (*k*+1), $\mathbf{S}_{k+1}^{-}$ according to (15) if SES is used, or update the smoothing levels and trends, $\mathbf{L}_k$ and $\mathbf{T}_k$ according to (17) if DES is used;
13) Set $k = k + 1$, and go to 1).

IV. Special Consideration for Distribution Systems

Different than transmission systems, a distribution system is typically an unbalanced one [18]. Its bus voltages or power flows on three phases are not balanced either. Therefore, for any bus, each phase needs to be modeled separately during its operation and control. The distributed generations and loads may be connected to a bus through either a DELTA-connection or a WYE-connection. Each load may contain constant-power components, constant-current components, and constant-impedance components. In this work, all load components and distributed generations are treated as constant powers. This may introduces some inaccuracy to the state estimation, but is acceptable for practical applications. More accurate and complicated models will be investigated in our future work.

The DELTA-connected generations, or loads [14] are converted to equivalent WYE-connected ones. The equivalent power injection at corresponding phase is determined based on the current between phases and the phase voltage at the phase. For example, a generation/load between phase x and phase y, $S_{i,x-y}$ can be converted into two equivalent generations/loads at phase x and phase y, $S_{i,x-y}^{x}$ and $S_{i,x-y}^{y}$ according to:

$$S_{i,x-y}^{x} = \frac{V_{i,x}e^{j\theta_{i,x}}}{V_{i,x}e^{j\theta_{i,x}} - V_{i,y}e^{j\theta_{i,y}}} S_{i,x-y},$$

$$S_{i,x-y}^{y} = \frac{-V_{i,y}e^{j\theta_{i,y}}}{V_{i,x}e^{j\theta_{i,x}} - V_{i,y}e^{j\theta_{i,y}}} S_{i,x-y}, \tag{22}$$

where, $V_{i,x}$ and $\theta_{i,x}$ are the magnitude and phase angle of voltage at bus i on phase x ; $V_{i,y}$ and $\theta_{i,y}$ are the magnitude and phase angle of voltage at bus i on phase y. The equivalent generation/load for any phase x that is connected with both WYE-connected and DELTA-connected generations/loads, $S_{i,x}^{EQ}$ can be determined as

$$S_{i,x}^{EQ} = S_{i,x} + \frac{V_{i,x}e^{j\theta_{i,x}}}{V_{i,x}e^{j\theta_{i,x}} - V_{i,y}e^{j\theta_{i,y}}} S_{i,x-y} - \frac{V_{i,x}e^{j\theta_{i,x}}}{V_{i,z}e^{j\theta_{i,z}} - V_{i,x}e^{j\theta_{i,x}}} S_{i,z-x}, \tag{23}$$

where, $S_{i,x}$ is the WYE-connected generation/load at phase x, $V_{i,z}$ and $\theta_{i,z}$ are the magnitude and phase angle of voltage at bus i on phase z, $S_{i,z-x}$ is the DELTA-connected generation/load between phases z and x. If assumed that voltages are balanced at the bus i, (22) and (23) can be further simplified as:

$$S_{i,x-y}^{x} = \frac{\sqrt{3}e^{-j30^o}}{3} S_{i,x-y}, \; S_{i,x-y}^{y} = \frac{\sqrt{3}e^{j30^o}}{3} S_{i,x-y}, \tag{24}$$

$$S_{i,x}^{EQ} = S_{i,x} + \frac{\sqrt{3}e^{-j30^o}}{3} S_{i,x-y} + \frac{\sqrt{3}e^{j30^o}}{3} S_{i,z-x}, \tag{25}$$

For any phase m of a bus i, its power injection can be determined according to:

$$S_{i,m} = S_{G_{i,m}}^{EQ} - S_{D_{i,m}}^{EQ}, \quad m \in PH^{i}, \tag{26}$$

where, $S_{i,m}$ is the power injection at phase m of bus i, $S_{G_{i,m}}^{EQ}$ is the equivalent generation output of generators at phase m of bus i, $S_{D_{i,m}}^{EQ}$ is the equivalent power demands of loads at phase m of bus i, and PH^{i} is the set of energized phases at bus i.

In the proposed method, the required power injection predictions for each phase of buses are determined based on the forecasts of equivalent distributed generation outputs and load demands that connected to the bus on the phase. After the power injections are determined, the backward-forward sweep algorithm can be employed to determine the voltages for all buses and the power flows for all branches. The algorithm consists of two basic steps, backward sweep and forward sweep, which are repeated until convergence is achieved. The backward sweep is primarily a process of power flow summation, and during the process, the voltages held constant and only branch power flows are updated. The forward sweep is primarily a process of voltage drop calculation, and during the process, the branch power flows held constant and only bus voltages are updated. The load flow computation can be achieved by two stages. In the first stage, (24)-(25) are used to get an initial solution. Then, (22) and (23) are used in the second stage to get the final solution.

The state variables for a distribution system are the voltage magnitudes and phase angles on each energized phase of buses in the system. The nodal power injections can be related to system state variables through the following nodal power flow equations:

$$S_{i,m} = V_{i,m}e^{j\theta_{i,m}} \left[\sum_{j\in BUS, n\in PH^{j}} \left(Y_{i,m-j,n}^{SYS} V_{j,n} e^{j\theta_{j,n}} \right)^{*} \right], \tag{27}$$

where, $S_{i,m}$ is the power injection at bus i on phase m. BUS is the bus set of the system, PH^{j} is the energized phase set at bus j; $V_{i,m}$ and $\theta_{i,m}$ are the voltage magnitude and phase angle at bus i on phase m ; $V_{j,n}$ and $\theta_{j,n}$ are the voltage magnitude and phase angle at bus j on phase n; $Y_{i,m-j,n}^{SYS}$ is the element of system admittance matrix at the row corresponding to bus i and phase m, and the column corresponding to bus j and phase n. The system admittance matrix $\mathbf{Y}^{SYS}$ can be determined according to the branch connections in the system, and corresponding admittance matrices for each branch.

In addition to the bus voltage and power injections, a distribution system typically measures power flows on some branches as well. For a two-terminal branch with impedance, the power flows at any phase of the branch can be determined according to the phase voltages at its terminal buses, and the admittance matrix for the branch:

$$S_{ij,m} = V_{i,m}e^{j\theta_{i,m}} \left[\sum_{n\in PH^{ij}} \left(Y_{i,m-i,n}^{ij} V_{i,n} e^{j\theta_{i,n}} + Y_{i,m-j,n}^{ij} V_{j,n} e^{j\theta_{j,n}} \right)^{*} \right],$$

$$S_{ji,m} = V_{j,m}e^{j\theta_{j,m}} \left[\sum_{n\in PH^{ij}} \left(Y_{j,m-i,n}^{ij} V_{i,n} e^{j\theta_{i,n}} + Y_{j,m-j,n}^{ij} V_{j,n} e^{j\theta_{j,n}} \right)^{*} \right], \tag{28}$$

where, $S_{ij,m}$ and $S_{ji,m}$ are the powers flowing from bus i towards bus j, and from bus j towards bus i on phase m of the branch respectively. $V_{i,n}$ and $\theta_{i,n}$ are the voltage magnitude and phase angle at bus i on phase n. $V_{j,m}$ and $\theta_{j,m}$ are the voltage magnitude and phase angle at bus j on phase m. PH^{ij} is the energized phase set for the branch between bus i and bus j. $Y_{i,m-i,n}^{ij}$, $Y_{i,m-j,n}^{ij}$, $Y_{j,m-i,n}^{ij}$ and $Y_{j,m-j,n}^{ij}$ are the elements of admittance matrix for the branch, $\mathbf{Y}^{ij}$ at the row and column given by the subscript letters, in which the first twos give the corresponding bus and phase of the row, and last twos give the corresponding bus and phase of the column. The admittance matrix $\mathbf{Y}^{ij}$ is used to define the relationship between the injected currents and voltages at each phase of terminals buses on the branch. The formulation of admittance matrix can be different for different types of branches. For a line segment, its admittance matrix is defined by its series impedances and shunt admittances. For a transformer, its admittance matrix is defined by its winding connections, tap positions, and impedances.

V. NUMERICAL EXAMPLES

To verify the effectiveness of the proposed method, multiple tests with different focus have been conducted. The test system used is modified from the IEEE 123-node test feeder [19]. As shown in Fig. 1, seven buses in the system have been modified to connect with photovoltaic (PV) generations, including bus 13, bus 35, bus 47, bus 57, bus 64, bus 76 and bus 101.

The tests were conducted based on simulation data. Fig. 2 gives the daily load and generation profile for the test system on a 3-minutes interval basis, thus for the tests shown afterwards, the estimation interval is also set to be 3 minutes. In Fig. 2, the horizontal represents the accumulated number of time intervals, and the vertical axis represents the corresponding scaling factors for loads and generations at each time interval with respect to the base generation and base load. The base power output for each PV generation is (20.0 + j 15.0) kVA per phase, and the loads for each bus given in [19] are treated as its base loads. The test results were obtained based on the data sets at intervals between 139 and 200, in which the data sets at intervals 139 and 140 are used to set the initial levels and trends for exponential smoothing algorithms. The parameters of exponential smoothing algorithms are set as: $\alpha_f = 0.3$, and $\beta_f = 0.2$. The parameters for unscented Kalman filters are set as [20]: $\alpha_s = 1.0, \kappa = 0$, and $\beta_s = 2.0$. The simulated data for load and generation forecast are determined as true load and generation profiles plus white noises. Meanwhile, the measurements are created through load flow calculations with true load and generation profiles plus white noises. The measurements used include active and reactive power injections at 56 buses, active and reactive power flows on 106 line segments, and voltage magnitudes on 20 buses. It is assumed that all measurements are provided by a SCADA system.

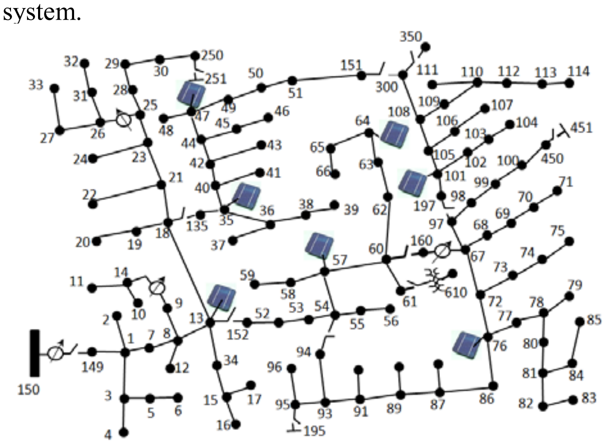

Fig. 1. A modified IEEE 123-node test feeder

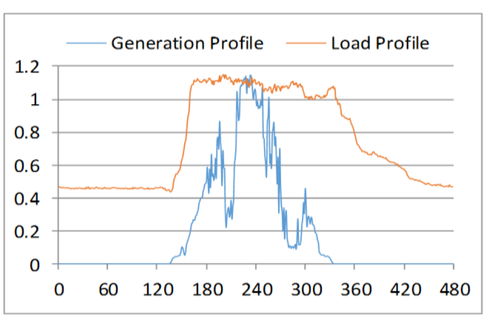

Fig. 2. Daily load and PV generation profile

The proposed method has been tested against different scenarios defined based on the levels of forecasting errors and state/measurement noises. Table I lists the standard deviation settings for three different testing scenarios. The standard deviations are defined at absolute values for phase angles and voltage magnitudes, but relative values for power injections or power flows. In Table I, the standard deviations of white noises for voltage magnitudes (per unit) and phase angles (radians) are set to be 0.01, 0.02 and 0.03, and for active and reactive powers are set to be 1%, 2% and 3% of their actual values respectively. Besides used for generating simulated data with noises for measurement and load and generation forecasting, the standard deviations of voltage magnitude and powers are also used to set the measurement covariance matrix, and the standard deviations of voltage magnitude and phase angles are used to set the state covariance for states. The state and measurement covariance matrices are diagonals.

Table I. Test Cases

Test Scenario	Standard Deviations			
	Voltage Magnitude (per unit)	*Phase Angle (radians)*	*Active Powers*	*Reactive Powers*
I	0.01	0.01	1%	1%
II	0.02	0.02	2%	2%
III	0.03	0.03	3%	3%

A. Improvement over State Forecasting based DSE

Firstly, the accuracy of the proposed method is compared against the ones using direct state forecasting. Four approaches using respectively SES and DES, direct state forecasting (marked by "-SF") and power injection forecasting (marked by "-PF") are compared using the mean absolute error (MAE) for state variables. The tests were run on an 8-core 3.20GHZ processor, and all algorithms were implemented using C language. Table II gives the average MAEs of estimated phase angles and voltage magnitudes for each approach. Table II also provides the average computation time for each approach to complete a single-interval state estimation. Fig. 3 and Fig. 4 show the variations of MAEs of estimated phase angles and voltage magnitudes across intervals between 140 and 200 for state forecasting based approaches and power injection forecasting based approaches, respectively. The test scenario I was applied to all approaches.

TABLE II. ESTIMATION ACCURACY COMPARISON OF FOUR APPRAOCHES

Approach	Test Scenario	Average MAE		Computation Time (Seconds)
		Phase Angle (radians)	*Voltage Magnitude (per unit)*	
SF-SES	I	0.01349	0.25545	15.9981
SF-DES	I	0.02559	0.29021	16.0526
PF-SES	I	0.00354	0.00344	22.2948
PF-DES	I	0.00310	0.00357	22.4363

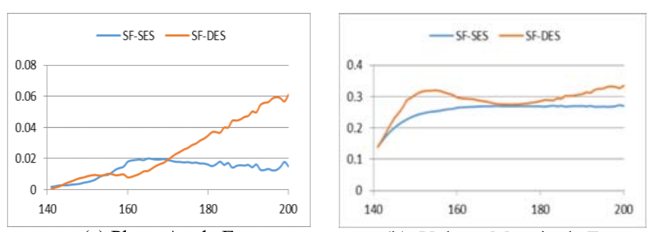

(a).Phase Angle Errors (b). Voltage Magnitude Errors

Fig. 3. MAEs of state estimations for direct state forecasting methods

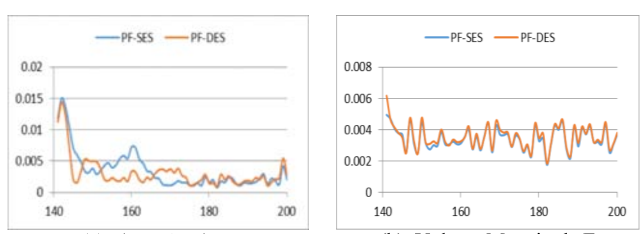

(a).Phase Angle Errors (b). Voltage Magnitude Errors

Fig. 4. MAEs of state estimations for power injection forecasting methods

It can be seen that the ones with power injection forecasting outperforms the other two. Compared with direct state forecasting ones, the computation time for power injection forecasting based approaches increased around 28.45%, but the estimation accuracy has been improved at least 4 times accurate than the direct forecasting ones. As for power injection forecasting approaches, the estimation accuracies achieved by DES-based forecasting and SES-based forecasting are almost at the same level.

B. Accuracy of the Proposed Method

The accuracy of the proposed method is compared under different testing scenarios using different types of exponential smoothing techniques. The results are given in Table III. The average MAEs of all state variables are used as the indicator to be compared.

TABLE III. COMPARISON OF AVERAGE MAES

Approach	**Test Scenario**	**Average MAE**	
		Phase Angle (radians)	***Voltage Magnitude (per unit)***
PF-SES	I	0.00354	0.00344
	II	0.03264	0.02301
	III	0.07068	0.08500
PF-DES	I	0.00310	0.00357
	II	0.01207	0.01666
	III	0.07895	0.13249

As demonstrated in Table III, the estimation accuracy is heavily affected by the accuracy levels of state modeling, measurement and forecasting. The larger the errors of state modeling, measurement and forecasting, the less accurate results the estimation can get. Under three different testing scenarios, the SES-based approaches still got results with comparable accuracy with DES-based ones. This can be explained by examining the load and generation profiles given in Fig. 2. As shown in Fig. 2, there are no distinct increasing/decreasing trends existing among time intervals. Therefore, the trend components used in DES-based approaches should not have big contributions to the accuracy of estimation.

C. Effects of Sanity Check and Adjustment for Power Injections

Table IV gives the test results obtained by using same scenarios as Table III, but the power injections were adjusted according to the results of sanity check. The ranges of rational power injection variations are set based on six times the standard deviations of injection noises. Comparing with Table III, it can be seen that the accuracy of state estimation for scenarios with larger standard deviations such as Scenario II, and Scenario III has been significantly improved when applying the sanity check and adjustment to the power injection forecasting.

Table IV. AVERAGE MAES WITH SANITY ADJUSTMENTS

Approach	**Test Scenario**	**Average MAE**	
		Phase Angle (radians)	***Voltage Magnitude (per unit)***
PF-SES	I	0.00251	0.00393
	II	0.00267	0.00495
	III	0.00288	0.00602
PF-DES	I	0.00216	0.00353
	II	0.00240	0.00463
	III	0.00270	0.00578

VI. CONCLUSIONS

This paper introduces very-short term load and DG injection forecasting into UKF-based DSE to improve the estimation accuracy of dynamic state estimation for distribution systems. The nodal power injections from load and DG are forecasted and transformed into state predictions through load flow computation. In addition, the sanity check and adjustment for power injections are used to mitigate the impacts of bad data and irrational sigma points on the estimation accuracy.

Future and ongoing research includes the investigation the impacts of the variability of reactive powers on the nodal power injection forecasts, load and distribution generation modeling, as well as the observability requirement analysis.

VII. REFERENCES

[1] A. Sinha and J. Mondal, "Dynamic state estimator using ANN based bus load prediction," *IEEE Transactions on Power Systems*, vol. 14, no. 4, pp. 1219–1225, 1999.

[2] D. Mallieu, T. Van Cutsem, P. Rousseaux, and M. Ribbens-Pavella,"Dynamic multilevel filtering for real-time estimation of electric power systems," *Control, Theory and Advanced Technology*, vol. 2, no. 2, 1986.

[3] P. Rousseaux, T. Van Cutsem, and T. D. Liacco, "Whither dynamic state estimation?" *International Journal of Electrical Power & Energy Systems*, vol. 12, no. 2, pp. 104–116, 1990.

[4] S. Sarri, M. Paolone, R. Cherkaoui, A. Borghetti, F. Napolitano, and C. A. Nucci, "State estimation of active distribution networks: comparison between WLS and iterated Kalman-filter algorithm integrating PMUs," in *Proc.* 2012 *3rd IEEE PES International Conference and Exhibition on Innovative Smart Grid Technologies Europe,*. pp. 1–8.

[5] E. Wan, R. Van Der Merwe et al., "The unscented Kalman filter for nonlinear estimation," in *Proc. 2000 IEEE Adaptive Systems for Signal Processing, Communications, and Control Symposium, pp. 153–158.*

[6] G. Valverde and V. Terzija, "Unscented Kalman filter for power system dynamic state estimation," *IET generation, transmission & distribution,* vol. 5, no. 1, pp. 29–37, 2011.

[7] E. Ghahremani and I. Kamwa, "Online state estimation of a synchronous unscented Kalman filter from phasor measurements units," *IEEE Transactions on Energy Conversion*, vol. 26, no. 4, pp. 1099– 1108, December 2011.

[8] S. Wang, W. Gao et al., "An alternative method for power system dynamic state estimation based on unscented transform," *IEEE Transactions on Power Systems*, vol. 27, no. 2, pp. 942–950, 2012.

[9] A. Rouhani and A. Abur, "Tracking the machine states using a linear phasor estimator assisted dynamic state estimator," in *Proc. 2014 IEEE PES General Meeting— Conference & Exposition*, pp. 1–5.

[10] A. S. Debs and R. Larson, "A dynamic estimator for tracking the state of a power system," *IEEE Transactions on Power Apparatus and Systems*, no. 7, pp. 1670–1678, 1970.

[11] A. L. Da Silva, M. B. Do Coutto Filho, and J. De Queiroz, "State forecasting in electric power systems," *IEE Proceedings C, Generation, Transmission and Distribution*, vol. 130, no. 5, pp. 237–244, 1983.

[12] P. Nguyen, G. K. Venayagamoorthy, W. Kling, and P. Ribeiro, "Dynamic state estimation and prediction for real-time control and operation," in *Proc.* 2013 *Clemson University Power System Conference*, pp.1-5.

[13] E. Blood, B. Krogh, and M. Ilic, "Electric power system static state estimation through Kalman filtering and load forecasting," in *Proc. 2008 IEEE PES General Meeting*, pp. 1–6.

[14] W. H. Kersting, *Distribution System Modeling and Analysis*(2nd ed), New York:CRC Press, 2007, pp.298-343.

[15] D. Shirmohammadi, H. W. Hong, A. Semlyen, and G. X. Luo, "A compensation-based power flow method for weakly meshed distribution and transmission networks," *IEEE Transactions on Power Systems*, vol. 3, no.2, pp.753-762, 1988.

[16] J. W. Taylor, "An evaluation of methods for very short-term load forecasting using minute-by-minute British data," *International Journal of Forecasting*, vol. 24, no. 4, pp. 645–658, 2008.

[17] E. S. Gardner, Jr. "Exponential smoothing: the state of the art – Part II", *International Journal of Forecasting*, vol. 22, no.4, pp. 637–666, 2006.

[18] Tsai-Hsiang Chen, Mo-Shing Chen, Kab-Ju Hwang, Paul Kotas, and Elie A. Chebli, "Distribution system power flow analysis - a rigid approach", *IEEE Transactions on Power Delivery*, vol. 6, no. 3, pp.1146-1152, July 1991.

[19] IEEE Distribution System Analysis Subcommittee. (2013) Distribution test feeders. [Online]. Available: http://ewh.ieee.org/soc/pes/dsacom/testfeeders/index.html

[20] S. Sarkka, "On unscented Kalman filtering for state estimation of continuous-time nonlinear systems", *IEEE Transactions on Automatic Control*, vol. 52, no. 9, pp. 1631–1641, 2007.